Binding Mode Analysis of 3-(4-Benzoyl-1-methyl-1*H*-2-pyrrolyl)-*N*-hydroxy-2-propenamide: A New Synthetic Histone Deacetylase Inhibitor Inducing Histone Hyperacetylation, Growth Inhibition, and Terminal Cell Differentiation

Antonello Mai,*,† Silvio Massa,‡ Rino Ragno,§ Monica Esposito,† Gianluca Sbardella,|| Giuseppina Nocca,⊥ Roberto Scatena,⊥ Florian Jesacher,# Peter Loidl,# and Gerald Brosch*,#

Dipartimento di Studi Farmaceutici, Università degli Studi di Roma "La Sapienza", P. le A. Moro 5, 00185 Roma, Italy, Dipartimento Farmaco Chimico Tecnologico, Università degli Studi di Siena, via A. Moro, 53100 Siena, Italy, Dipartimento di Studi di Chimica e Tecnologia delle Sostanze Biologicamente Attive, Università degli Studi di Roma "La Sapienza", P. le A. Moro 5, 00185 Roma, Italy, Dipartimento di Scienze Farmaceutiche, Università degli Studi di Salerno, via Ponte Don Melillo, 84084 Fisciano (SA), Italy, Istituto di Biochimica e Biochimica Clinica, Università Cattolica del Sacro Cuore, L. go F. Vito 1, 00168 Roma, Italy, and Department of Microbiology, Medical School, University of Innsbruck, Fritz-Pregl-Strasse 3, 6020 Innsbruck, Austria

Received November 2, 2001

The binding mode of 3-(4-aroyl-1*H*-2-pyrrolyl)-*N*-hydroxy-2-propenamides **1a**−**c**, belonging to a recently reported class of synthetic histone deacetylase (HDAC) inhibitors (Massa, S.; et al. *J. Med. Chem*. **2001**, *44*, 2069−2072), into the new modeled HDAC1 catalytic core is presented, and enzyme/inhibitor interactions are discussed. HDAC1 X-ray coordinates were obtained by virtual "mutation" of those of histone deacetylase-like protein, a bacterial HDAC homologue. In in vitro antimaize HD2 as well as antimouse HDAC1 assay, compounds **1a**−**c** showed inhibitory activities in the low micromolar range. Similarly, **1a**−**c** are endowed with anti-HDAC activity in vivo: on mouse A20 cells, **1a**−**c** induced histone hyperacetylation leading to a highly increased acetylation level of H4 as compared to control histones. Results obtained with acid−urea−triton polyacrylamide gel electrophoresis have been confirmed by Western Blot experiments. Finally, compound **1a**, chosen as a representative member of this class of HDAC inhibitors, resulted endowed with antiproliferative (45 and 85% cell growth inhibition at 40 and 80 μM, respectively) and cellular differentiation (18 and 21% of benzidine positive cells at the same concentrations) activities in murine erythroleukemic cells.

Introduction

Histone deacetylases (HDACs) represent a family of enzymes that compete with histone acetyltransferases (HATs) to modulate chromatin structure and transcriptional activity via changes in the acetylation status of nucleosomal histones.[1] Histones H2A, H2B, H3, and H4 exhibit acetyl groups at the ϵ-amino-terminal lysine residues within the tails extending from the histone octamer of the nucleosome core. Among them, histones H3 and H4 constitute the main targets of HDAC enzymatic activity.[2−5] Gene transcription or repression is associated with the ability of transcriptionally competent genes to recruit either HAT or HDAC proteins to the promoter.[6] Association of HATs with transcription factor complexes results in acetylation of histones and neutralization of the positive charge on their lysine residues, allowing nucleosomal relaxation and subsequent gene transcription.[7−10] Conversely, transcriptional repression occurs when HDACs are recruited to transcription cofactors, such as Mad/Max,[11] Rb and Rb-like proteins,[12−14] unliganded hormone receptors,[15] N-CoR,[16,17] or SMRT.[15] These complexes remove the acetyl groups restoring the positive charge on lysine side chains of histones. The result is a tightness of nucleosomal integrity and gene silencing.

In the last 10 years, a number of HDAC inhibitors have been reported as useful tools to study the function of chromatin acetylation and deacetylation and gene expression. Among them, trichostatin A (TSA),[18] a cyclic tetrapeptide family including trapoxin (TPX),[19] chlamydocin,[20] HC toxin,[21] Cyl-2,[22] WF-3161,[23] and apicidin,[24] and the more recent depsipeptide FK-228 (FR901228)[25] have been isolated from cultures of fungal strains (Chart 1). Differently, sodium butyrate (NaB),[26] suberoyl anilide hydroxamic acid (SAHA) and the related second generation hybrid polar compounds (HPCs),[27] amide analogues of TSA,[28] and benzamide derivatives with MS-27-275 as the lead compound[29] were obtained by synthetic pathways (Chart 1).

Recently, we have reported a new group of synthetic HDAC inhibitors, namely, 3-(4-aroyl-1*H*-2-pyrrolyl)-*N*-hydroxy-2-propenamides (APHAs).[30] Three-dimensional (3D) structure-based drug design and molecular modeling studies based upon the X-ray crystal structure of a bacterial HDAC homologue (histone deacetylase-like

* To whom correspondence should be addressed. A. M., Tel.: +396-4991-3392. Fax: +396-491-491. E-mail: antonello.mai@uniroma1.it. G. B., Tel.: 0512-507-3608. Fax: 0512-507-2866. E-mail: gerald.brosch@uibk.ac.at.

† Dipartimento di Studi Farmaceutici, Università degli Studi di Roma "La Sapienza".

‡ Università degli Studi di Siena.

§ Dipartimento di Studi di Chimica e Tecnologia delle Sostanze Biologicamente Attive, Università degli Studi di Roma "La Sapienza".

|| Università degli Studi di Salerno.

⊥ Università Cattolica del Sacro Cuore.

University of Innsbruck.

10.1021/jm011088+ CCC: $22.00
Published on Web 03/26/2002

Chart 1. Structure of Known Histone Deacetylase Inhibitors

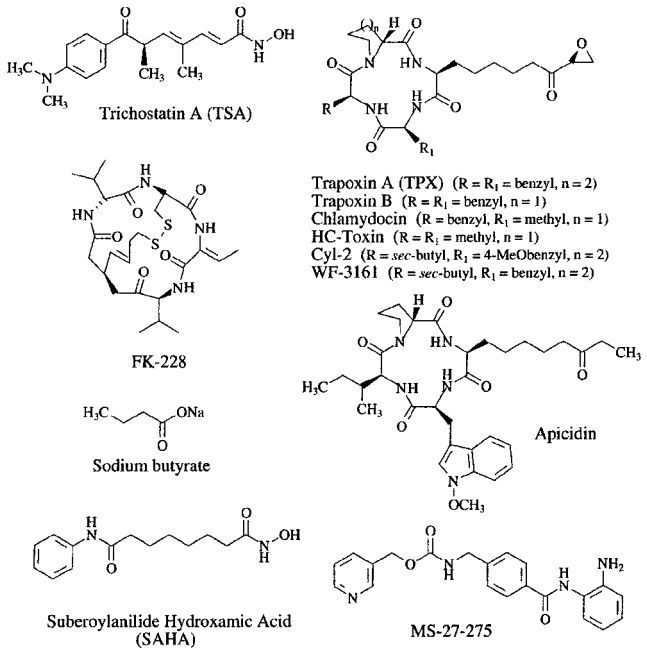

protein, HDLP)[31] prompted us to evaluate the HDAC inhibitory activity of previously reported[32,33] and newly synthesized pyrrole derivatives, leading us to discover a new class of compounds endowed with HDAC (maize histone deacetylase HD2) inhibitory activity in the low micromolar range. The most active derivative **1b** (IC_{50} = 1.9 μM) shows a 500-fold higher inhibitory potency than NaB and a 264-, 38-, 190-, and 17-fold lower potency than TSA, SAHA, TPX, and HC toxin, respectively.[30]

In the present study, to better define the binding mode of APHA derivatives into the deacetylase catalytic core, HDAC1 X-ray coordinates were obtained by virtual "mutation" of those of HDLP, and selected APHA compounds **1a**−**c** were tested against mouse HDAC1 enzyme in vitro.

Furthermore, in vivo HDAC inhibitory activity of **1a**−**c** through histone hyperacetylation assay and growth inhibition and terminal cell differentiation properties of **1a** chosen as a representative member of APHA class were also determined.

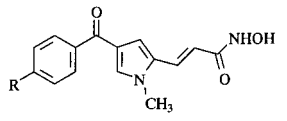

1a R = H
1b R = CH_3
1c R = $N(CH_3)_2$

Chemistry

Compounds **1a**,**b** were prepared as previously reported by us.[32,33] The synthesis of **1c** was accomplished by reaction of ethyl 3-[4-(4-*N*,*N*-dimethylaminobenzoyl)-1-methyl-1*H*-2-pyrrolyl]-2-propenoate (**2**)[32] with hydroxylamine hydrochloride and potassium hydroxide. Alternately, treatment of 3-[4-(4-*N*,*N*-dimethylaminobenzoyl)-1-methyl-1*H*-2-pyrrolyl]-2-propenoic acid (**3**)[32] with ethyl chloroformate and triethylamine followed by addition

Scheme 1[a]

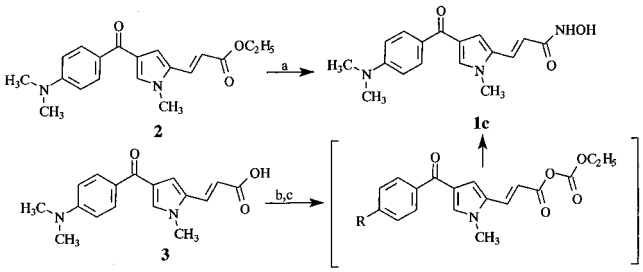

[a] Reagents: (a) KOH, NH_2 OH, HCl. (b) ClCOOEt, Et_3N. (c) NH_2OH.

of freshly prepared hydroxylamine afforded the desired compound **1c** (Scheme 1).

Binding Mode Analysis. Because the inhibitors **1a**−**c** were tested against the maize HD2,[30,34−37] the use of HDLP 3D coordinates to estimate their binding mode may result in little accuracy due to the differences existing between the two enzymes. For modeling purposes, the optimum situation would be the virtual mutation of the catalytic core of HDLP to that of HD2. Unfortunately, the low homology sequence degree existing between HDLP and HD2[38] does not allow this transformation in a feasible computational way. On the contrary, a high degree of homology is reported to exist between HDLP and HDAC1.[31] Therefore, we decided to model the deacetylase catalytic core of HDAC1 from the HDLP coordinates (Protein Data Bank entry code 1c3r)[31,39] and to test **1a**−**c** against mouse HDAC1 enzyme using TSA and SAHA as reference drugs.[40]

Starting from the HDLP/TSA complex, we modeled the HDAC1 catalytic core by mutation of all of the HDLP residues comprised in a shell of 12 Å from the cocrystallized TSA. In the new modeled HDAC1/TSA complex, the replacement of TSA with **1a**, chosen as a representative member of the APHA class, furnished a new complex, which was used to refine the binding mode of our derivatives into the HDAC1 pocket. The VALIDATE paradigm[30,41] was employed as a scoring tool to select the **1a** optimum binding geometry from an ensamble of 216 pregenerated conformations.

In Vivo HDAC Activity Inhibition and Terminal Cell Differentiation. Many HDAC inhibitors have been shown to induce cell accumulation of hyperacetylated histones H3 and H4.[18,19,27−29,42−45] Histone hyperacetylation is directly linked to the activation of p21 transcription (elevated $p21^{waf1}$ expression) and is p53-independent.[45] Moreover, histone hyperacetylation causes cell cycle arrest and growth inhibition acting in concert with other growing regulatory pathways.[46] In in vitro inhibitory assay, compounds **1a**−**c** showed anti-HD2 activity in the low micromolar range (Figure 1).[30] When tested against mouse HDAC1, **1a**−**c** displayed IC_{50} values similar to those obtained against HD2 (Table 1).[40]

To investigate whether in vitro HDAC inhibition correlates with increased acetylation level of core histones in vivo, exponentially growing A20 cells were treated with different concentrations of **1a**−**c**, together with TSA and SAHA as reference drugs, and the analysis of histone hyperacetylation by AUT-PAGE (acid−urea−triton polyacrylamide gel electrophoresis) followed by staining with Coomasie brilliant blue R-250 was performed. Highly acetylated histone H4 isoforms

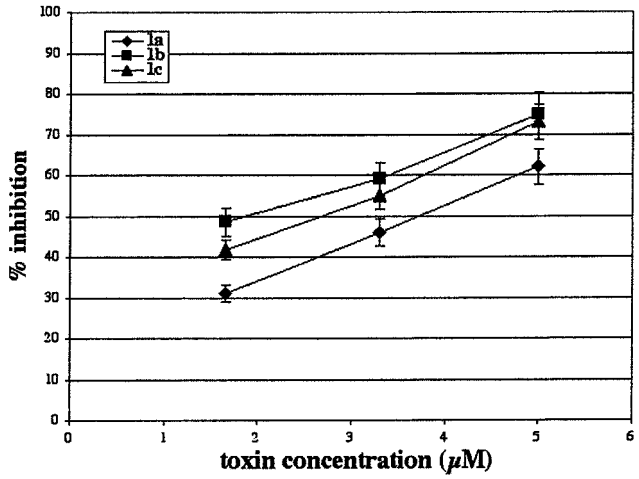

Figure 1. In vitro HD2 inhibitory activity of **1a**−**c**.

Table 1. Anti-HDAC Activity of Compounds **1a**−**c**

compd	anti-HD2 $IC_{50} \pm SD$ (μM)[a]	anti-HDAC1 $IC_{50} \pm SD$ (μM)
1a	3.8 ± 4%	4.9 ± 3%
1b	1.9 ± 3%	4.5 ± 4%
1c	2.4 ± 3%	4.2 ± 4%
TSA	0.007 ± 4%	0.002 ± 3%
SAHA	0.05 ± 3%	0.112 ± 4%

[a] See ref 30.

(di-, tri-, and tetraacetylated) were immunodetected by Western Blot analysis.

The treatment of cancer by differentiation factors is growing up in clinical studies. Cytodifferentiating agents induce the neoplastic cells to remove their maturation blockage allowing them to develop toward more differentiated cell types.

Because a link between HDAC inhibition and induction of differentiation of several cancer cell lines has been recently established,[24,27,28,47−51] the potential of the prototype of APHA class (**1a**) as inducer of growth inhibition and differentiation in Friend leukemia cells was explored in comparison with TSA and SAHA.

Results and Discussion

Binding Mode Investigation and Molecular Modeling Studies. We built the HDAC1 catalytic core starting from the HDLP/TSA complex[31] as described in the Experimental Section. In the new modeled HDAC1/TSA complex, the replacement of TSA with **1a**, chosen as a representative member of the APHA class, furnished a new complex, which was used to study the APHA binding mode into the HDAC1 catalytic core (Figure 2). The VALIDATE paradigm was employed as a scoring tool to select the **1a** binding mode from a family of 216 pregenerated conformations. The modeling of **1b**,**c** structures from the **1a** binding conformation and the optimal recalculation of the **1a**−**c** pK_i values by the VALIDATE application confirmed the selected binding geometry (Table 2). The VALIDATE procedure, applied on the new modeled HDAC1/**1a**−**c** complexes, afforded lower average absolute error of prediction (AAEP) than that observed for the corresponding HDLP/**1a**−**c** counterparts ($AAEP_{HDAC1} = 0.28$ pK_i vs $AAEP_{HDLP} = 0.99$ pK_i).

An inspection of HDAC1/**1a**−**c** complexes shows that the hydroxamic acid moiety of APHA inhibitors resulted slightly far from the catalytic zinc ion (CO−Zn, 4.5 Å; OH−Zn, 4.8 Å) for producing efficient metal chelation, whereas the related groups of SAHA and TSA were positioned to the optimal bond distance (CO_{SAHA}−Zn, 2.91 Å; OH_{SAHA}−Zn, 3.14 Å; CO_{TSA}−Zn, 2.92 Å; OH_{TSA}−Zn, 3.13 Å) for zinc ion complexing (Figure 2). This effect is probably due to a steric hindrance exerted by the pyrrole N_1-methyl group into the binding pocket. This group lies on the same protein cavity the TSA C-6-(*R*)-methyl group fits (side chains of PHE198 and LEU265). However, the pyrrole N_1-methyl produces a sticking of **1a**−**c** into the catalytic pocket so that the APHA CONHOH group cannot get the optimal CO−Zn and OH−Zn bond distances for ion complexing. This blockage is also supported by the interactions made by the aroyl portions of **1a**−**c** into a hydrophobic cavity with the TYR91 benzyl- and the ASP92 β-CH_2 side chains.

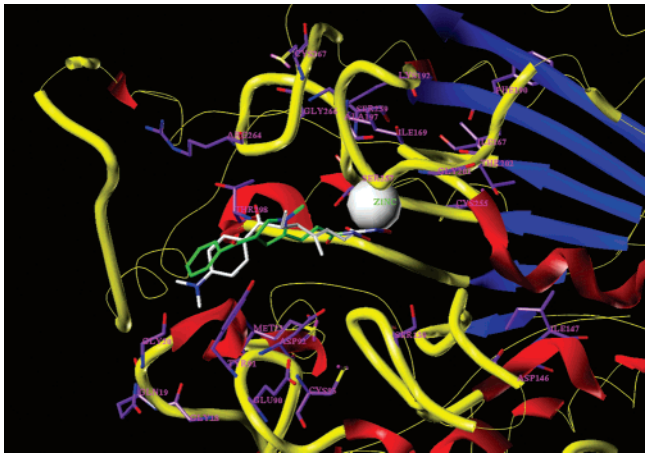

Figure 2. Three-dimensional model of **1a** docked into the HDAC1 catalytic core. Compound **1a** is in green, TSA is in white, and the mutated HDLP → HDAC1 residues are in purple. α-Carbon atom trace of the HDAC/HDLP structure is in yellow. A 15 Å core from TSA is shown in the tube/ribbon graphic.

Table 2. Experimental vs VALIDATE-Predicted Anti-HDAC Activities of **1a**−**c**

compd	HD2 expt pK_i[a]	mouse HDAC1 expt pK_i[a]	HDAC1 predicted pK_i	HDLP predicted pK_i
1a	5.64	5.53	5.76	6.52
1b	5.95	5.57	5.83	7.02
1c	5.84	5.60	5.68	6.89
TSA	8.36	8.97	8.61	8.66
SAHA	6.88	7.17	6.69	6.27

[a] Experimental pK_i values of **1a**−**c** and SAHA were obtained by the corresponding IC_{50} values in comparison with the pK_i and IC_{50} values of TSA.[30,52]

Histone Hyperacetylation Assay. Exponentially growing mouse A20 cells were treated with different concentrations of compounds **1a**−**c** together with TSA and SAHA as references. After isolation of nuclei, extracted histones were separated on AUT gels and stained with Coomassie blue. AUT-PAGE allows the separation of individual acetylated subspecies especially of H4 as a result of HDAC inhibition. Figure 3 shows that all of our synthetic inhibitors induced the accumulation of highly acetylated H4 forms. As a result, a clear shift from non- and monoacetylated to di- and triacetylated histone H4 subspecies can be observed, as compared to control in which no toxin was added. As previously demonstrated,[18,27] treatment of cells with

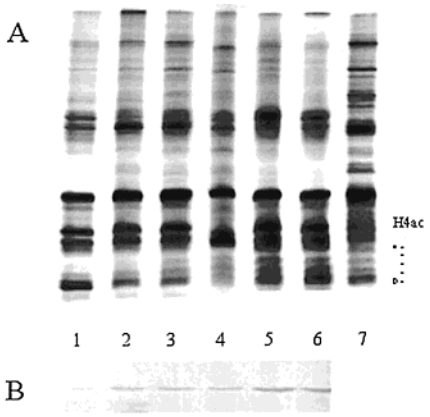

Figure 3. Effects of **1a**−**c**, TSA, and SAHA on histone acetylation in mouse A20 cells. (A) Analysis of histone hyperacetylation by AUT-PAGE and Coomassie blue staining. Positions of mono- up to tetraacetylated H4 subspecies are indicated. (1) control (no toxin added to cells), (2) **1c**, (3) **1a**, (4) **1b**, (5) TSA, (6) SAHA, (7) hyperacetylated MEL cell histones. (B) Western Blot analysis of H4 acetylation. Position of acetylated H4 is indicated.

TSA and SAHA, two highly specific inhibitors of HDAC, causes hyperacetylation of histone H4 (Figure 3A).

Furthermore, antibodies that recognize di-, tri-, and tetraacetylated histone H4, but not nonacetylated H4 N-terminal peptides, have been used as a probe for agents that cause histone hyperacetylation. In Western Blot experiments, isolated histones of Figure 3A were subjected to sodium dodecyl sulfate (SDS)−PAGE and immunoblotting. Treatment of cells with **1a**−**c** as well as with TSA and SAHA leads to a highly increased acetylation level of H4 as compared to control histones; all tested compounds gave a significant immunoreaction whereas in control only a very faint signal is visible (Figure 3B). Joined to AUT-gel results, these data clearly indicate that our synthetic compounds are specific inhibitors of HDAC activity in vivo.

Growth Inhibition and Cytomorphological Murine Erythroleukemic (MEL) Cell Line Differentiation. In addition to the in vitro and in vivo HDAC inhibition assay, the capability of **1a** to induce antiproliferative effects and cell differentiation in Friend MEL cells has been investigated. These cells are known to respond to HDAC inhibitors with hemoglobin accumulation that can be visualized and quantified by benzidine staining.[51,27] Figure 4A shows the effect of different HDAC inhibitors on cell growth of MEL cells, cultured for 48 h. All compounds showed a significant dose-dependent inhibitory effect on the growth rate of the cell line ($p < 0.01$). In particular, cell growth inhibition resulted in 40 and 67% for TSA at 15 and 30 nM, 52 and 80% for SAHA at 0.6 and 1.2 μM, and 45 and 85% for **1a** at 40 and 80 μM, respectively. Interestingly, after 48 h, the inhibitors were not cytotoxic at the lower tested concentrations. Only SAHA at 1.2 μM and **1a** at 80 μM were shown to induce a significant cytotoxic effect (20.5 and 19.5% cell death, respectively; vehicle, 5.3% cell death) (graphic not shown).

In MEL cells, the hemoglobin accumulation, revealed by benzidine staining, is linked to activation of the differentiation process. The results (Figure 4B) clearly indicate a dose-dependent increase of hemoglobin synthesis for all compounds tested, showing that **1a** is able

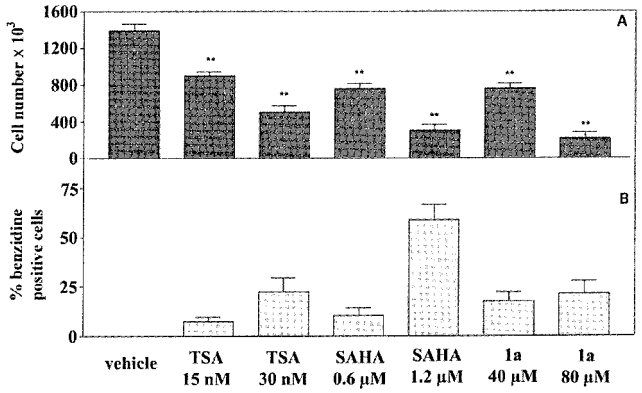

Figure 4. Growth inhibition and cell differentiation effects of **1a** on MEL cell line. (A) Effect of **1a** on cell growth of MEL cells, cultured for 48 h. TSA and SAHA are used as reference drugs. Data are expressed as cell number (mean ± SEM, $n = 4$); **, $p < 0.01$. (B) Concentration-dependent effects of **1a**, TSA, and SAHA on differentiation of MEL cells. The cells were cultured with various concentrations of drugs for 96 h. Each point is the mean ± SEM ($n = 4$); *, $p < 0.05$; **, $p < 0.01$.

to induce cell differentiation in MEL cells with 18 and 21% of benzidine positive cells at 40 and 80 μM. SAHA at 1.2 μM induces the larger increment in hemoglobin synthesis (benzidine positive cells were about 60%).

Experimental Section

Chemistry. Melting points were determined on a Büchi 530 melting point apparatus and are uncorrected. Infrared (IR) spectra (KBr) were recorded on a Perkin-Elmer 310 instrument. ^{1}H nuclear magnetic resonance (NMR) spectra were recorded at 200 MHz on a Bruker AC 200 spectrometer; chemical shifts are reported in δ (ppm) units relative to the internal reference tetramethylsilane (Me_4Si). All compounds were routinely checked by thin-layer chromatography (TLC) and ^{1}H NMR. TLC was performed on aluminum-backed silica gel plates (Merck DC-Alufolien Kieselgel 60 F_{254}) with spots visualized by UV light. All solvents were reagent grade and, when necessary, were purified and dried by standard methods. Concentration of solutions after reactions and extractions involved the use of a rotary evaporator operating at a reduced pressure of ca. 20 Torr. Organic solutions were dried over anhydrous sodium sulfate. Analytical results are within ±0.40% of the theoretical values. A SAHA sample for biological assays was prepared as previously reported by us.[53] All chemicals were purchased from Aldrich Chimica, Milan (Italy), or Lancaster Synthesis GmbH, Milan (Italy), and were of the highest purity.

Synthesis of 1c from 2. To a hydroxylamine hydrochloride (1.95 g, 28.1 mmol) solution in dry ethanol (10 mL), a potassium hydroxide (1.58 g, 28.1 mmol) solution in dry ethanol (10 mL) was added at 40 °C. The mixture was cooled at 0 °C and then filtered, and to the clear solution, **2**[32] (1.00 g, 3.1 mmol) and well-crushed potassium hydroxide (292 mg, 5.2 mmol) were added. After 4 h, the mixture was diluted with water (50 mL), made neutral with 0.1 N HCl, and filtered under vacuum. The solid was collected, dried, and recrystallized by 2-propanol. Yield, 50%; mp 184−185 °C. IR: 3150 (NHOH), 1640 (CONH), 1590 (CO) cm^{-1}. ^{1}H NMR (DMSO-d_6): δ 2.95 (s, 6 H, $N(CH_3)_2$), 3.70 (s, 3 H, NCH_3), 6.25 (d, 1 H, CH=C*H*CO), 6.70 (d, 2 H, benzene H-3,5), 6.83 (s, 1 H, pyrrole β-proton), 7.33 (d, 1 H, C*H*=CHCO), 7.48 (s, 1 H, pyrrole α-proton), 7.68 (d, 2 H, benzene H-2,6), 9.00 (s, 1 H, NH), 10.50 (s, 1 H, OH). Anal. Calcd ($C_{17}H_{19}N_3O_3$): C, 65.16%; H, 6.11%; N, 13.41%. Found: C, 65.03; H, 6.10%; N, 13.58%.

Synthesis of 1c from 3. To a 0 °C cooled solution of **3**[32] (1.00 g, 3.3 mmol) in dry tetrahydrofuran (20 mL), ethyl chloroformate (0.45 mL, 4.5 mmol) and triethylamine (0.70 mL, 4.8 mmol) were added and the mixture was stirred for 10 min. The solid was filtered off, and the filtrate was added to freshly

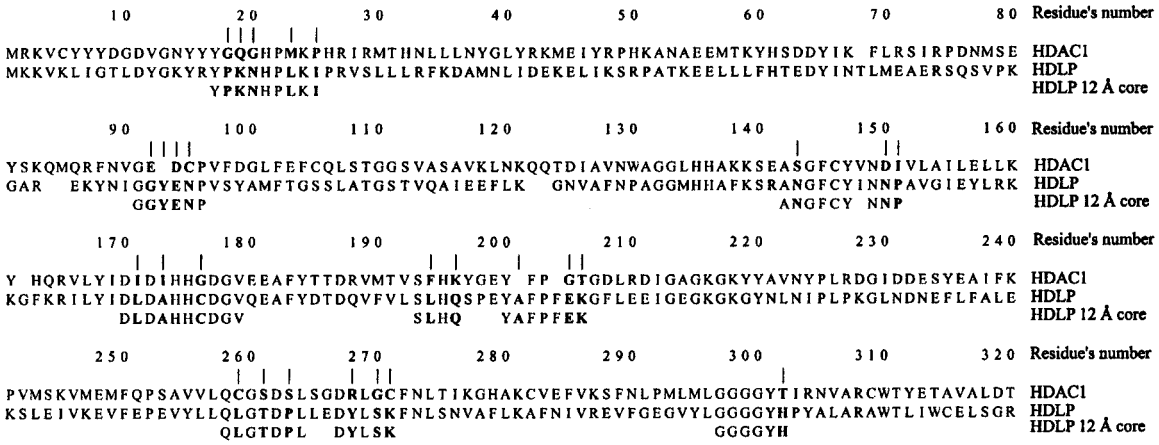

Figure 5. Sequence alignment of HDAC1, HDLP, and HDLP-12 Å core.

prepared hydroxylamine[54] (0.18 g, 5.6 mmol) in methanol. The resulting mixture was stirred at room temperature for 15 min and then was evaporated, and the residue was recrystallized from 2-propanol to give a sample of **1c** identical to that obtained by the previously described method. Yield, 54%.

Computational Studies. All molecular modeling calculations and manipulations were performed using the software packages Macromodel 6.5,[55] SYBYL 6.5,[56] MOPAC 2000,[57,58] VALIDATE,[41] GOLPE 4.5,[59] Swiss PDB Viewer[60] running on Silicon Graphics O2 R10000 and IBM compatible Pentium IV 1.4 GHz workstations.

The crystal structure of TSA extracted from the HDLP/TSA complex filed in the Brookhaven Protein Data Bank[31,39] (entry code 1c3r) was used as a template to build the 3D structures of **1a**−**c**. The HDAC1 model was constructed from HDLP by mutating (MUTATE command in the Swiss PDB Viewer) all of the residues comprised in a shell of 12 Å from the cocrystallized TSA. Figure 5 shows the sequence alignment of HDAC1, HDLP, and HDLP 12 Å core. The HDAC1 residue sequence was taken from the Swiss-Prot database[61] and scored a 36.5% identity with the crystallized HDLP sequence, using the default setting in SYBYL for sequence alignment.

Replacement of TSA with the modeled compounds **1a**−**c** in the HDAC1 catalytic core afforded three new complexes, which were geometrically optimized (MACROMODEL 6.5, all atoms Amber force field).[55,62,63] Although available in the MACROMODEL program, a solvation model for this minimization was not used; however, the numerous water molecules from the original 1c3r PDB complex were retained during the minimization. For the molecular alignment of **1a**−**c** into the enzyme, an atom by atom superimposition was employed, based on the hydroxamic portions of TSA and APHA derivatives.

Compound **1a** was used for the APHA binding mode refinement. To this purpose, a family of 216 conformations of **1a** was generated using the following semiautomatic docking procedure: the initial conformation of **1a** obtained from the HDAC1/**1a** minimized complex was arbitrarily rotated by a step of 10 degrees along an axis passing through the center of the benzene ring and the hydroxamic carbon atom. Each of the obtained new 36 complexes was submitted to a grid search rotating the four dihedral angles by a step of 30 degrees (Figure 6). By filtering out all of the complexes showing a molecular clashing between **1a** and the enzyme pocket, the final conformation family was achieved.

The selection of the most probable binding conformation of **1a** was based on energy criteria upon minimization of the new 216 HDAC1/**1a** complexes (global minimum). A second selection was based on the application of a modified version of the VALIDATE procedure,[64] which was used to recalculate the **1a** K_i value associated with each modeled complex. The HDAC1/**1a** global minimum conformation exactly coincided with that producing the lowest error of K_i prediction by VALIDATE. Binding conformations of **1b**,**c** were directly modeled from the selected **1a** binding conformation and submitted to geometry optimization with the program MACROMODEL. Analogue procedure was also performed using HDLP enzyme coordinates in order to make a direct comparison of the results obtained with HDAC1 coordinates.

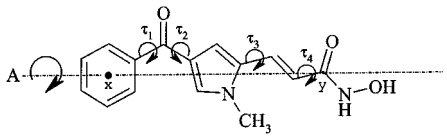

Figure 6. Semiautomatic docking procedure generating a family of 216 conformations of **1a**. A represents the axis of rotation passing through the center (*x*) of the benzene ring and the hydroxamic carbon atom (*y*). τ_1−τ_4 indicate the four rotatable bonds used for the grid searches.

In Vitro Anti-mHDAC1 Assay. For inhibition assays, partially purified HDAC1 from mouse A20 cells (ATCC: TIB-208) (anion exchange chromatography, affinity chromatography (Jesacher and Loidl, unpublished results)) was used as the enzyme source. HDAC activity was determined as described[40] using [^{3}H]acetate prelabeled chicken reticulocyte histones as substrate. A 50 μL amount of mouse HDAC1 was incubated with different concentrations of compounds for 15 min on ice, and 10 μL of total [^{3}H]acetate prelabeled chicken reticulocyte histones (4 mg/mL) was added, resulting in a concentration of 41 μM. This mixture was incubated at 37 °C for 1 h. The reaction was stopped by addition of 50 μL of 1 M HCl/0.4 M acetylacetate and 1 mL of ethyl acetate. After centrifugation at 10 000*g* for 5 min, an aliquot of 600 μL of the upper phase was counted for radioactivity in 3 mL of liquid scintillation cocktail.

In Vivo Histone Hyperacetylation. Mouse A20 cells were maintained in RPMI 1640 medium at 37 °C and 5% CO_2. Exponentially growing cells were incubated for 8 h with **1a**−**c** at final concentrations of 800, 400, and 500 μM, respectively. As references, cells were also treated with TSA (200 nM) and SAHA (11 μM). After incubation, cells were washed and harvested by centrifugation. Isolation of nuclei, extraction of histones, and analysis of histone hyperacetylation by AUT-PAGE followed by staining with Coomasie brilliant blue R-250 were performed according to standard procedures.[65,66] Hyperacetylation was also investigated by immunoblotting. For this purpose, equal amounts of isolated histones (estimated by laser densitometry) were electrophoresed in precast 14% SDS−PAGE and blotted onto a nitrocellulose membrane. Membrane strips were incubated with an antibody against acetylated peptide corresponding to the amino acids 2−19 of *Tetrahymena* histone H4 (Upstate Biotechnology, USA). This antibody recognizes highly acetylated histone H4 isoforms (di-, tri-, and tetraacetylated). Immunodetection was performed using secondary antibody alkaline phosphatase conjugates.

Growth Inhibition and Cell Differentiation Assay. Cell Culture and Reagents. MEL cells were obtained from Interlab Cell Line Collection (CBA) (Genoa, Italy). Cells were

maintained at 37 °C under a humidified atmosphere of 5% CO_2 in RPMI 1640 Hepes modified medium supplemented with 10% (v/v) heat-inactivated fetal calf serum, 2 mmol/L glutamine, 100 IU/mL penicillin, and 100 μg/mL streptomycin. Unless indicated, all chemicals and reagents (cell culture grade) were obtained from Sigma Chemical Co., Milan, Italy.

Cell Viability and Growth Inhibition Assay. Cell number was determined using a Neubauer hemocytometer, and viability was assessed by their ability to exclude trypan blue. The stock solutions were prepared immediately before use. TSA, SAHA, and **1a** were dissolved in DMSO. MEL exponentially growing cells (1×10^5 cells/mL) were set at day 0 in media containing various concentrations of drugs for 96 h. The final concentrations of the drugs were as follows: TSA, 15 and 30 nM; SAHA, 0.6 and 1.2 μM; **1a**, 40 and 80 μM. The final concentration of DMSO, used as vehicle, was the same (0.1% v/v) in all samples during the experiments.

Cytomorphological Assay for MEL Cell Differentiation. The most widely used method for scoring erythroid differentiation is benzidine staining, which reveals the production of hemoglobin.[67] Benzidine dihydrochloride (2 mg/mL) was prepared in 3% acetic acid. Hydrogen peroxide (1%) was added immediately before use. The MEL cell suspensions were mixed with the benzidine solution in a 1:1 ratio and counted in a hemocytometer after 5 min. Blue cells were considered to be positive for hemoglobin.

Statistical Analysis. All results are expressed as mean ± SEM. The group means were compared by analysis of variance (ANOVA) followed by a multiple comparison of means by Dunnet test. $p < 0.05$ was considered significant.

Acknowledgment. We thank A. Loidl for expert technical assistance. This work was supported in part by an APART-fellowship from the Austrian Academy of Sciences to G.B.

References

(1) Emiliani, S.; Fischle, W.; Van Lint, C.; Al-Abed, Y.; Verdin, E. Characterization of a human RPD3 ortholog, HDAC3. *Proc. Natl. Acad. Sci. U.S.A.* **1998**, *95*, 2795−2800.
(2) Grunstein, M. Histone acetylation in chromatin structure and transcription. *Nature* **1997**, *389*, 349−352.
(3) Hebbes, T. R.; Thorne, A. W.; Crane-Robinson, C. A direct link between core histone acetylation and transcriptionally active chromatin. *EMBO J.* **1988**, *7*, 1395−1402.
(4) Loidl, P. Histone Acetylation: facts and questions. *Chromosoma* **1994**, *103*, 441−449.
(5) Tazi, J.; Bird, A. Alternative chromatin structure at CpG islands. *Cell* **1990**, *60*, 909−920.
(6) Saunders, N. A.; Popa, C.; Serewko, M. M.; Jones, S. J.; Dicker, A. J.; Dahler, A. L. Histone deacetylase inhibitors: novel anticancer agents. *Exp. Opin. Invest. Drugs* **1999**, *8*, 1611−1621.
(7) Mizzen, C. A.; Yang, X. J.; Kokubo, T.; Brownell, J. E.; Bannister, A. J.; Owen-Hughes, T.; Workman, J.; Wang, L.; Berger, S. L.; Kouzarides, T.; Nakatani, Y.; Allis, C. D. The TAF(II)250 subunit of TFIID has histone acetyltransferase activity. *Cell* **1996**, *87*, 1261−1270.
(8) Ogryzko, V. V.; Schiltz, R. L.; Russanova, V.; Howard, B. H.; Nakatani, Y. The transcriptional coactivators p300 and CBP are histone acetyltransferases. *Cell* **1996**, *87*, 953−959.
(9) Bannister, A. J.; Kouzarides, T. The CBP co-activator is a histone acetyltransferase. *Nature* **1996**, *384*, 641−643.
(10) Struhl, K. Histone acetylation and transcriptional regulatory mechanisms. *Genes Dev.* **1998**, *12*, 599−606.
(11) Laherty, C. D.; Yang, W.-M.; Sun, J.-M.; Davie, J. R.; Seto, E.; Eisenman, R. N. Histone deacetylases associated with the mSin3 corepressor mediate mad transcriptional repression. *Cell* **1997**, *89*, 349−456.
(12) Brownell, J. E.; Zhou, J.; Ranalli, T.; Kobayashi, R.; Edmondson, D. G.; Roth, S. Y.; Allis, C. D. Tetrahymena histone acetyltransferase A: a homologue to yeast Gcn5p linking histone acetylation to gene activation. *Cell* **1996**, *84*, 843−851.
(13) Ferreira, R.; Magnaghi-Jaulin, L.; Robin, P.; Harel-Bellan, A.; Trouche, D. The three members of the pocket proteins family share the ability to repress E2F activity through recruitment of a histone deacetylase. *Proc. Natl. Acad. Sci. U.S.A.* **1998**, *95*, 10493−10498.
(14) Stiegler, P.; De Luca, A.; Bagella, L.; Giordano, A. The COOH-terminal region of pRb2/p130 binds to histone deacetylase 1 (HDAC1), enhancing transcriptional repression of the E2F-dependent cyclin A promoter. *Cancer Res.* **1998**, *58*, 5049−5052.
(15) Nagy, L.; Kao, H.-Y.; Chakravarti, D.; Lin, R. J.; Hassig, C. A.; Ayer, D. E.; Schreiber, S. L.; Evans, R. M. Nuclear receptor repression mediated by a complex containing SMRT, mSin3A, and histone deacetylase. *Cell* **1997**, *89*, 373−380.
(16) Alland, L.; Muhle, R.; Hou, H.; Potes, J.; Chin, L.; Schreiber-Agus, N.; DePinho, R. A. Role for N-CoR and histone deacetylase in Sin3-mediated transcriptional repression. *Nature* **1997**, *387*, 49−55.
(17) Heinzel, T.; Lavinsky, R. M.; Mullen, T.-M.; Soderstrom, M.; Laherty, C. D.; Torchia, J.; Yang, W.-M.; Brard, G.; Ngo, S. D.; Davie, J. R.; Seto, E.; Eisenman, R. N.; Rose, D. W.; Glass, C. K.; Rosenfeld, M. G. A complex containing N-CoR, mSin3 and histone deacetylase mediates transcriptional repression. *Nature* **1997**, *387*, 43−48.
(18) Yoshida, M.; Kijima, M.; Akita, M.; Beppu, T. Potent and Specific Inhibition of Mammalian Histone Deacetylase both In Vivo and In Vitro by Trichostatin A. *J. Biol. Chem.* **1990**, *265*, 17174−17179.
(19) Kijima, M.; Yoshida, M.; Suguta, K.; Horinouchi, S.; Beppu, T. Trapoxin, an Antitumor Cyclic Tetrapeptide, Is an Irreversible Inhibitor of Mammalian Histone Deacetylase. *J. Biol. Chem.* **1993**, *268*, 22429−22435.
(20) Closse, A.; Hugenin, R. Isolation and structure elucidation of chlamydocin. *Helv. Chim. Acta* **1974**, *57*, 533−545.
(21) Shute, R. E.; Dunlap, B.; Rich, D. H. Analogues of the Cytostatic and Antimitogenic Agents Chlamydocin and HC-Toxin: Synthesis and Biological Activity of Chloromethyl Ketone and Diazomethyl Ketone Functionalized Cyclic Tetrapeptides. *J. Med. Chem.* **1987**, *30*, 71−78.
(22) Hirota, A.; Suzuki, A.; Aizawa, K.; Tamura, S. Mass spectrometric determination of amino acid sequence in Cyl-2, a novel cyclotetrapeptide from *Cylindrocladium scoparium*. *Biomed. Mass Spectrom.* **1974**, *1*, 15−19.
(23) Umehara, K.; Nakahara, K.; Kiyoto, S.; Iwami, M.; Okamoto, M.; Tanaka, H.; Kohsaka, M.; Aoki, H.; Imanaka, H. Studies on WF-3161, a new antitumor antibiotic. *J. Antibiot.* **1983**, *36*, 478−483.
(24) Han, J. W.; Ahn, S. H.; Park, S. H.; Wang, S. Y.; Bae, G. U.; Seo, D. W.; Known, H. K.; Hong, S.; Lee, Y. W.; Lee, H. W. Apicidin, a histone deacetylase inhibitor, inhibits proliferation of tumor cells via induction of p21WAF1/Cip1 and gelsolin. *Cancer Res.* **2000**, *60*, 6068−6074.
(25) Ueda, H.; Nakajima, H.; Hori, Y.; Fujita, T.; Nishimura, M.; Goto, T.; Okuhara, M. FR901228, a novel antitumor bicyclic depsipeptide produced by *Chromobacterium violaceum* No. 968. I. Taxonomy, fermentation, isolation, physicochemical and biological properties, and antitumor activity. *J. Antibiot.* **1994**, *47*, 301−310.
(26) Kruh, J. Effects of Sodium Butyrate, a New Pharmacological Agent, on Cells in Culture. *Mol. Cell. Biochem.* **1982**, *42*, 65−82.
(27) Richon, V. M.; Emiliani, S.; Verdin, E.; Webb, Y.; Breslow, R.; Rifkind, R. A.; Marks, P. A. A class of hybrid polar inducers of transformed cell differentiation inhibits histone deacetylases. *Proc. Natl. Acad. Sci. U.S.A.* **1998**, *95*, 3003−3007.
(28) Jung, M.; Brosch, G.; Kölle, D.; Scherf, H.; Gerhäuser, C.; Loidl, P. Amide Analogues of Trichostatin A as Inhibitors of Histone Deacetylase and Inducers of Terminal Cell Differentiation. *J. Med. Chem.* **1999**, *42*, 4669−4679.
(29) Suzuki, T.; Ando, T.; Tsuchiya, K.; Fukazawa, N.; Saito, A.; Mariko, Y.; Yamashita, T.; Nakanishi, O. Synthesis and Histone Deacetylase Inhibitory Activity of New Benzamide Derivatives. *J. Med. Chem.* **1999**, *42*, 3001−3003.
(30) Massa, S.; Mai, A.; Sbardella, G.; Esposito, M.; Ragno, R.; Loidl, P.; Brosch, G. 3-(4-Aroyl-1*H*-pyrrol-2-yl)-*N*-hydroxy-2-propenamides, a New Class of Synthetic Histone Deacetylase Inhibitors. *J. Med. Chem.* **2001**, *44*, 2069−2072.
(31) Finnin, M. S.; Donigian, J. R.; Cohen, A.; Richon, V. M.; Rifkind, R. A.; Marks, P. A.; Breslow, R.; Pavletich, N. P. Structures of a histone deacetylase homologue bound to the TSA and SAHA inhibitors. *Nature* **1999**, *401*, 188−193.
(32) Massa, S.; Artico, M.; Corelli, F.; Mai, A.; Di Santo, R.; Cortes, S.; Marongiu, M. E.; Pani, A.; La Colla, P. Synthesis and Antimicrobial and Cytotoxic Activities of Pyrrole-Containing Analogues of Trichostatin A. *J. Med. Chem.* **1990**, *33*, 2845−2849.
(33) Corelli, F.; Massa, S.; Stefancich, G.; Mai, A.; Artico, M.; Panico, S.; Simonetti, N. Ricerche su composti antibatterici ed antifungini. Nota VIII − Sintesi ed attività antifungina di derivati pirrolici correlati con la tricostatina A. (Researches on antibacterial and antifungal agents. VIII. Synthesis and antifungal activity of thricostatin A-related pyrrole derivatives.) *Farmaco, Ed. Sci.* **1987**, *42*, 893−903.
(34) Brosch, G.; Lusser, A.; Goralik-Schramel, M.; Loidl, P. Purification and characterization of a high molecular weight histone deacetylase complex (HD2) of maize embryos. *Biochemistry* **1996**, *35*, 15907−15914.

(35) Kölle, D.; Brosch, G.; Lechner, T.; Pipal, A.; Helliger, W.; Taplick, J.; Loidl, P. Different types of maize histone deacetylases are distinguished by a highly complex substrate and site specificity. *Biochemistry* **1999**, *38*, 6769−6773.
(36) Lechner, T.; Lusser, A.; Brosch, G.; Eberharter, A.; Goralik-Schramel, M.; Loidl, P. A comparative study of histone deacetylases of plant, fungal and vertebrate cells. *Biochim. Biophys. Acta* **1996**, *1296*, 181−188.
(37) Brosch, G.; Ransom, R.; Lechner, T.; Walton, J.; Loidl, P. Inhibition of maize histone deacetylases by HC toxin, the host-selective toxin of Cochliobolus carbonum. *Plant Cell* **1995**, *33*, 1941−1950.
(38) Khochbin, S.; Wolffe, A. P. The origin and utility of histone deacetylases. *FEBS Lett.* **1997**, *419*, 157−160.
(39) Bernstein, F. C.; Koetzle, T. F.; Williams, G. J. B.; Meyer, E. F., Jr.; Brice, M. D.; Rodgers, J. R.; Kennard, O.; Shimanouchi, T.; Tasumi, T. The Protein Data Bank: A Computer Based Archival File for Macromolecular Structures. *J. Mol. Biol.* **1977**, *112*, 535−542.
(40) In vitro anti-HDAC1 activity was determined by us (see Experimental Section) as described in Sendra, R.; Rodrigo, I.; Salvador, M. L.; Franco, L. Characterization of pea histone deacetylases. *Plant Mol. Biol.* **1988**, *11*, 857−866.
(41) Head, R. D.; Smythe, M. L.; Oprea, T. I.; Waller, C. L.; Green, S. M.; Marshall, G. R. VALIDATE: A New Method for the Receptor-Based Prediction of Binding Affinities of Novel Ligands. *J. Am. Chem. Soc.* **1996**, *118*, 3959−3969.
(42) Kwon, H. J.; Owa, T.; Hassig, C. A.; Shimada, J.; Schreiber, S. L. Depudecin induces morphological reversion of transformed fibroblasts via the inhibition of histone deacetylase. *Proc. Natl. Acad. Sci. U.S.A.* **1998**, *95*, 3356−3361.
(43) Vidali, G.; Boffa, C.; Bradbury, E. M.; Allfrey, V. G. Butyrate suppression of histone deacetylation leads to accumulation of multiacetylated forms of histones H3 and H4 and increased DNase I sensitivity of the associated DNA sequences. *Proc. Natl. Acad. Sci. U.S.A.* **1978**, *75*, 2239−2243.
(44) Zhou, Q.; Melkoumian, Z. K.; Lucktong, A.; Moniwa, M.; Davie, J. R.; Strobl, J. S. Rapid Induction of Histone Hyperacetylation and Cellular Differentiation in Human Breast Tumor Cell Lines following Degradation of Histone Deacetylase-1. *J. Biol. Chem.* **2000**, *275*, 35256−35263.
(45) Sambucetti, L. C.; Fischer, D. D.; Zabludoff, S.; Kwon, P. O.; Chamberlin, H.; Trogani, N.; Xu, H.; Cohen, D. Histone Deacetylase Inhibition Selectively Alters the Activity and Expression of Cell Cycle Proteins Leading to Specific Chromatin Acetylation and Antiproliferative Effects. *J. Biol. Chem.* **1999**, *274*, 34940−34947.
(46) Brinkmann, H.; Dahler, A. L.; Popa, C.; Serewko, M. M.; Parsons, P. G.; Gabrielli, B. G.; Burgess, A. J.; Saunders, N. A. Histone Hyperacetylation Induced by Histone Deacetylase Inhibitors Is Not Sufficient to Cause Growth Inhibition in Human Dermal Fibroblasts. *J. Biol. Chem.* **2001**, *276*, 22491−22499.
(47) Saito, A.; Yamashita, T.; Mariko, Y. Nosaka, Y.; Tsuchiya, K.; Ando, T.; Suzuki, T.; Tsuruo, T.; Nakanishis, O. A synthetic inhibitor of histone deacetylase, MS-27-275, with marked in vivo antitumor activity against human tumors. *Proc. Natl. Acad. Sci. U.S.A.* **1999**, *96*, 4592−4597.
(48) Archer, S. Y.; Meng, S.; Shel, A.; Hodin, R. A. p21WAF1 is required for butyrate-mediated growth inhibition of human colon cancer cells. *Proc. Natl. Acad. Sci. U.S.A.* **1998**, *95*, 6791−6796.
(49) Janson, W.; Brandner, G.; Siegel, J. Butyrate modulates DNA-damage-induced p53 response by induction of p53-independent differentiation and apoptosis. *Oncogene* **1997**, *15*, 1395−1406.
(50) Saunders, N. A.; Dicker, A.; Popa, C.; Jones, S.; Dahler, A. Histone Deacetylase Inhibitors as Potential Anti-Skin Cancer Agents. *Cancer Res.* **1999**, *59*, 399−404.
(51) Yoshida, M.; Nomura, S.; Beppu, T. Effects on trichostatins on differentiation of murine erythroleukemia cells. *Cancer Res.* **1987**, *47*, 3688−3691.
(52) Cheng, Y. C.; Prusoff, W. H. Relationship between the inhibition constant (K_i) and the concentration of inhibitor which causes 50% inhibition (IC_{50}) of an enzymatic reaction. *Biochem. Pharmacol.* **1973**, *22*, 3099−3108.
(53) Mai, A.; Esposito, M.; Sbardella, G.; Massa, S. A new facile and expeditious synthesis of *N*-hydroxy-*N*′-phenyloctanediamide, a potent inducer of terminal cytodifferentiation. *Org. Prep. Proced. Int.* **2001**, *33*, 391−394.
(54) Hydroxylamine hydrochloride (0.39 g, 5.6 mmol) in methanol (10 mL) was added to a stirred solution of potassium hydroxide (313 mg, 5.6 mmol) in methanol (10 mL) at 0 °C. After it was stirred for 15 min, the precipitate was removed and the filtrate was used as such.
(55) Mohamadi, F.; Richards, N. G. J.; Guida, W. C.; Liskamp, R.; Lipton, M.; Caufield, C.; Chang, G.; Hendrickson, T.; Still, W. C. MACROMODEL − an integrated software system for modeling organic and bioorganic molecules using molecular mechanics. *J. Comput. Chem.* **1990**, *11*, 440−467.
(56) *SYBYL*; Tripos Associates, Inc.: 1699 S. Hanley Rd, St. Louis, MO 63144.
(57) Stewart, J. J. MOPAC: a semiempirical molecular orbital program. *J. Comput.-Aided Mol. Des.* **1990**, *4*, 1−105.
(58) *MOPAC 2000.00 Manual*; Stewart, J. J. P., Ed; Fujitsu Limited: Tokyo, Japan, 1999.
(59) *GOLPE*. Multivariate Infometric Analysis Srl.: Viale dei Castagni 16, Perugia, Italy, 1999.
(60) Guex, N.; Peitsch, M. C. SWISS-MODEL and the Swiss-PdbViewer: an environment for comparative protein modeling. *Electrophoresis* **1997**, *18*, 2714−2723.
(61) Bairoch, A.; Apweiler, R. The SWISS−PROT protein sequence data bank and its supplement TrEMBL. *Nucleic Acids Res.* **1997**, *25*, 31−36 (http://www.ebi.ac.uk/ebi_docs/swissprot_db/swiss-home.html).
(62) Pearlman, D. A.; Case, D. A.; Caldwell, J. W.; Ross, W. S.; Cheatham, T. E., III; Debolt, S.; Ferguson, D. M.; Seibel, G. L.; Kollman, P. A. AMBER, a Package of Computer Programs for Applying Molecular Mechanics, Normal-Mode Analysis, Molecular Dynamics and Free Energy Calculations to Simulate the Structural and Energetic Properties of Molecules. *Comput. Phys. Commun.* **1995**, *91*, 1−41.
(63) Pearlman, D. A.; Case, D. A.; Caldwell, J. W.; Ross, W. S.; Cheatham, T. E., III; Ferguson, D. M.; Seibel, G. L.; Singh, U. C.; Weiner, P. K.; Kollman, P. A. *AMBER 4.1*; Department of Pharmaceutical Chemistry, University of California: San Francisco, CA, 1995.
(64) Manuscript in preparation. Briefly, the original VALIDATE procedure was modified by applying semiempirical AM1 calculated charges (keyword MOZYME in MOPAC 2000) to the training set and prediction set complexes. The use of such atomic charges improved the predictability of the VALIDATE method toward those complexes that involve proteins or enzymes containing metal cations, as in the case of HDLP/HDAC1. This VALIDATE model has been obtained using 86 ligand/protein complexes including the HDAC1/TSA complex.
(65) Alfageme, C. R.; Zweidler, A.; Mahowald, A.; Cohen, L. H. Histones of Drosophila embryos. Electrophoretic isolation and structural studies. *J. Biol. Chem.* **1974**, *249*, 3729−3736.
(66) Kölle, D.; Brosch, G.; Lechner, T.; Lusser, A.; Loidl, P. Biochemical methods for analysis of histone deacetylases. *Methods* **1998**, *15*, 323−331.
(67) Rowley, P. T.; Ohlsson-Wilhelm, B. M.; Farley, B. A.; La Bella, S. Inducers of erythroid differentiation in K562 human leukemia cells. *Exp. Hematol.* **1981**, *9*, 32−37.

JM011088+